Toughening Poly(lactic acid) with Imidazolium-based Elastomeric Ionomers

Li Pan

Quanzhou University of Economics and Trade

Abstract Imidazolium-based elastomeric ionomers (*i*-BIIR) were facilely synthesized by ionically modified brominated poly(isobutylene-*co*-isoprene) (BIIR) with different alkyl chain imidazole and thoroughly explored as novel toughening agents for poly(lactic acid) (PLA). The miscibility, thermal behavior, phase morphology and mechanical property of ionomers and blends were investigated through dynamic mechanical analyses (DMA), differential scanning calorimetry (DSC), scanning electron microscopy (SEM), tensile and impact testing. DMA and SEM results showed that better compatibility between the PLA and *i*-BIIR was achieved compared to the PLA/unmodified BIIR elastomer. A remarkable improvement in ductility with an optimum elongation at break up to 235% was achieved for the PLA/*i*-BIIR blends with 1-dodecylimidazole alkyl chain (*i*-BIIR-12), more than 10 times higher than that of pure PLA. The impact strengths of PLA were enhanced from 1.9 kJ/m^2 to 4.1 kJ/m^2 for the PLA/10 wt% *i*-BIIR-12 blend. Toughening mechanism had been established by systematical analysis of the compatibility, intermolecular interaction and phase structures of the blends. Interfacial cavitations initiated massive shear yielding of the PLA matrix owing to a suitable interfacial adhesion which played a key role in the enormous toughening effect in these blends. We believed that introducing imidazolium group into the BIIR elastomer was vital for the formation of a suitable interfacial adhesion.

Keywords Imidazolium-based ionomer; Poly(lactic acid); Brominated poly(isobutylene-*co*-isoprene); Toughening; Blend

INTRODUCTION

In recent years, sustainable polymers derived from renewable resource have attracted lots of attention because of the increasing concern over plastic pollution and petroleum resources shortages[1, 2]. Poly(lactic acid) (PLA) is one kind of the most successful bioplastic products derived from 100% renewable feedstocks in market. PLA shows good biocompatibility, excellent biodegradability, high mechanical strength, elasticity *etc*. These appealing properties make it a very promising alternative to petroleum-based plastic in wide applications ranging from packaging, texture and fiber to durable goods applications[3–6]. However, pure PLA is originally brittle with very low impact strength and elongation at break. The poor toughness and flexibility greatly hinder its wide and diverse commodity applications. Accordingly, considerable efforts have been devoted to developing PLA-based materials with high toughness.

Because of the advantages of simple, cost-effective, facile scale production and good industrial application prospect, melt blending PLA with other flexible polymers is a very promising and effective strategy for improving the mechanical properties of PLA. Rubber, flexible bioplastic and new synthesized polymers have been widely employed as modifiers for effective toughening PLA in some reported works[7–13]. Among these reported modifiers, the elastomers, such as natural rubber and poly(epichlorohydrin-*co*-ethylene oxide)[7, 14], have proven to be effective toughening agents to enhance the toughness and flexibility of PLA. However, the immiscibilitybetween the elastomeric components and PLA usually results in phase separation and poor interfacial adhesion, thereby reducing the physical properties of the material. Consequently, improving the compatibility between the PLA and the elastomer is a key issue to achieve high performance of PLA/elastomer blend. Several methods have been developed to improve the compatibility of PLA blend, including reactive melt-blending[15, 16], adding block or graft copolymer[17], and introducing intermolecular interaction[9, 18–23]. Recent research demonstrated that introducing intermolecular interaction, such as hydrogen bonding, dipole-dipole interaction, and ion interaction, is a very effective approach to improve the miscibility of polymer

blend. For example, Zhang's group systematically investigated metal cation ionomer as toughening agent and reactive compatilizer for PLA blend. They found that the incorporation of metal cation (Zn^{2+}) ionomer effectively improved the toughness of PLA matrix[21–23].

Some small ionic liquid (IL) molecules with organic cations, such as phosphonium-based ILs[24, 25] and imidazolium-based ILs[26–30] *etc*., were also investigated as plasticizers or compatilizers for the PLA and its blends. Recently, ionically modified elastomers have gained increasing interest in developing new materials with attractive properties, especially for the imidazolium-based ILs. We synthesized novel copolymers containing the imidazoliumcations to develop new polymer materials with interesting self-sealing behavior[31]. Other reports also proved that the introduction of imidazolium cations could give elastomer new properties due to the ionic interaction[32–35]. However, to the best of our knowledge, few reports focused on using elastomeric ionomers with organic cations as toughening agents or compatilizers for the PLA-based blend and composites. In this work, we synthesized a series of elastomeric imidazolium cations-based ionomers through facile reaction of brominated poly-(isobutylene-*co*-isoprene) (BIIR) with alkyl imidazole[33, 34]. These imidazolium cations-modified BIIRs (*i*-BIIR) were studied as toughening agents for PLA by melt blending method. The effects of intermolecular interaction, ionic aggregation and side alkyl chain on the interfacial compatibility, phase morphology, mechanical properties and toughening mechanisms were herein explored.

EXPERIMENTAL

Materials

Poly(lactic acid) (PLA, 3001D) was purchased from NatureWorks Inc, U. S. A. Brominated poly(isobutylene-*co*-isoprene) (BIIR, BB2030, 1.8 wt% Br, ~0.15 mmol allylic bromide functionality/g BIIR) was purchased from LANXESS Inc, Germany. PLA and BIIR were dried in vacuo prior to melt processing. Imidazole (99%), 1-ethylimidazole (98%), 1-butylimidazole (98%), 1-bromooctane (99%) and 1-bromododecane (99%) were used as received from J&K Scientific LTD, China.

Synthesis of Monomers and Ionomers

Synthesis of1-octylimidazole and 1-dodecylimidazole

Alkylimi-dazole monomers were synthesized by imidazole and alkyl bromide referring to the previous report[36]. Imidazole (6.81 g, 100 mmol), 1-bromooctane (19.32 g, 100 mmol), NaOH (50 wt% in deionized water) (8.8 g, 110 mmol) were mixed with tetrahydrofuran (40 mL). Upon dissolving, the solution was heated to 65 °C andrefluxed for 3 days. After cooling to r.t., the solvent was removed by rotary evaporation. The crude product was extracted three times with dichloromethane and deionized water. The organic layer was then dried with magnesium sulfate. After concentrated by rotary evaporation, the crude product was purified by column chromatography with ethyl acetate as eluent. The ethyl acetate was removed by rotary evaporation to give 1-octylimidazole as a pale-yellow oil in 87.2% yield. ^{1}H-NMR (400 MHz, $CDCl_3$, δ, ppm): 7.46 (s, 1H, −N−C<u>H</u> −N−), 7.05 (s, 1H, −N−C<u>H</u> =CH−N−), 6.90 (s, 1H, −N−CH =C<u>H</u> −N−), 3.92 (t, 2H, C<u>H</u>$_2$), 1.77 (m, 2H, C<u>H</u>$_2$), 1.34–1.24 (m, 10H, C<u>H</u>$_2$), 0.88 (t, 3H, C<u>H</u>$_3$).

Another monomer, 1-dodecylimidazole was synthesized *via* a similar process, and obtained as a pale-yellow oil in a yield of 84.6%. ^{1}H-NMR (400 MHz, $CDCl_3$, δ, ppm): 7.46 (s, 1H, −N−C<u>H</u> −N−), 7.05 (s, 1H, −N−C<u>H</u> = CH−N−), 6.90 (s, 1H, −N−CH =C<u>H</u> −N−), 3.92 (t, 2H, C<u>H</u>$_2$), 1.77 (m, 2H, C<u>H</u>$_2$), 1.31–1.24 (m, 18H, C<u>H</u>$_2$), 0.88 (t, 3H, C<u>H</u>$_3$).

Synthesis ofbrominated poly(isobutylene-co-isoprene) ionomers

Brominated poly(isobutylene-*co*-isoprene) ionomer was synthesized by quaternization[37, 38]. BIIR (30.0 g, 4.5 mmol allylic bromide functionality) was dissolved in toluene (100 mL) into a 1000 mL three-necked round bottom flask. The solution was heated to 90 °C till all rubber was dissolved. 1-Ethylimidazole (4.41 g, molar ratio of Br/imidazole monomer is 1/6) was added to the reaction mixture under nitrogen. The viscous mixture was stirred and heated to 110 °C, refluxed for 12 h. After that, the mixture was cooled to r.t., precipitated into acetone and washed for 3 times. After removing the solvent in a vacuum oven at 50 °C for 24 h, the creamy-white product, *i*-BIIR-2 was obtained in 98% yield. The *i*-BIIR-4, *i*-BIIR-8, and *i*-BIIR-12 were synthesized *via* a similar process. The structure of the ionomers was determined by a Bruker 400 MHz spectrometer (400 MHz, $CDCl_3$) and analyzed later.

Preparation of Blends

Melt blends were prepared by using a Haake batch intensive mixer (Haake Rheomix 600, Germany) with a batch volume of 60 mL at a screw speed of 60 r/min for 6 min at 180 °C. During the mixing process, the torque was continuously monitored. PLA was mechanically mixed with BIIR and *i*-BIIR-4 from 5 wt% to 30 wt%, respectively. To explore the impact of different alkyl chain lengths on the PLA/*i*-BIIR blends, PLA was mechanically mixed with *i*-BIIR-2, *i*-BIIR-8, and *i*-BIIR-12 at the same proportion of 10 wt%, respectively. Similarly, the neat PLA was subjected to the mixing treatment to have the same thermal history. PLA, BIIR and *i*-BIIR were dried in vacuo at 70 °C for 24 h prior to melt blending.

The detailed physical and analytical measurements were described in the electronic supplementary information (ESI).

RESULTS AND DISCUSSION

Synthesis and Characterization of Brominated Elastomeric Ionomers

Firstly, we synthesized imidazole monomers with different alkyl chain lengths *via* a pathway in Scheme 1. 1-Octylimidazole and 1-dodecylimidazole monomers were obtained in high yield anddefinitely characterized by ^{1}H-NMR spectra, respectively (Fig. S1 in ESI). The short-length imidazole monomers were commercially available. *i*-BIIR ionomers with ≥ 0.90 conversion of grafting degree were

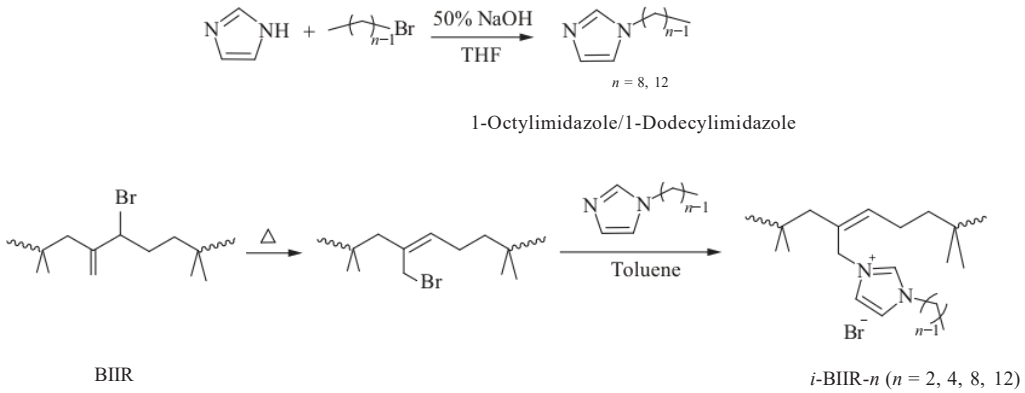

Scheme 1 Synthesis of imidazole monomers and imidazoliumbrominatedelastomeric ionomers

successfully obtained by facile and efficient quaternization reaction of these obtained imidazole monomers and BIIR[34].

^{1}H-NMR spectra were used to characterize the structure of the synthesized ionomers. As shown in Fig. 1, the resonance signals at 4.96 ppm (H9) and 4.89 ppm (H12) were assigned to the protons of imidazolium in the imidazolium cations modified BIIR. These were used to calculate the conversion of quaternary reaction (results are presented in Table1). Signal at 5.1 ppm (H1) was assigned to non-brominated isoprene units. Signals of H2–H4 were almost completely diminished and weak signals of H5 and H7 demonstrated the high degree of ionization. ^{1}H-NMR spectra of other ionomers, including *i*-BIIR-2, *i*-BIIR-8 and *i*-BIIR-12 are presented in Fig. S2 (in ESI). All the spectroscopic data obtained were in good agreement with the previous reported results[33, 34].

The thermal andrheological behaviors of BIIR and *i*-BIIR were investigated by DSC, DMA, TGA and rheological measurements, respectively, since these properties are very important for the processing and performance of PLA/elastomer blends. All samples displayed similar T_gs around

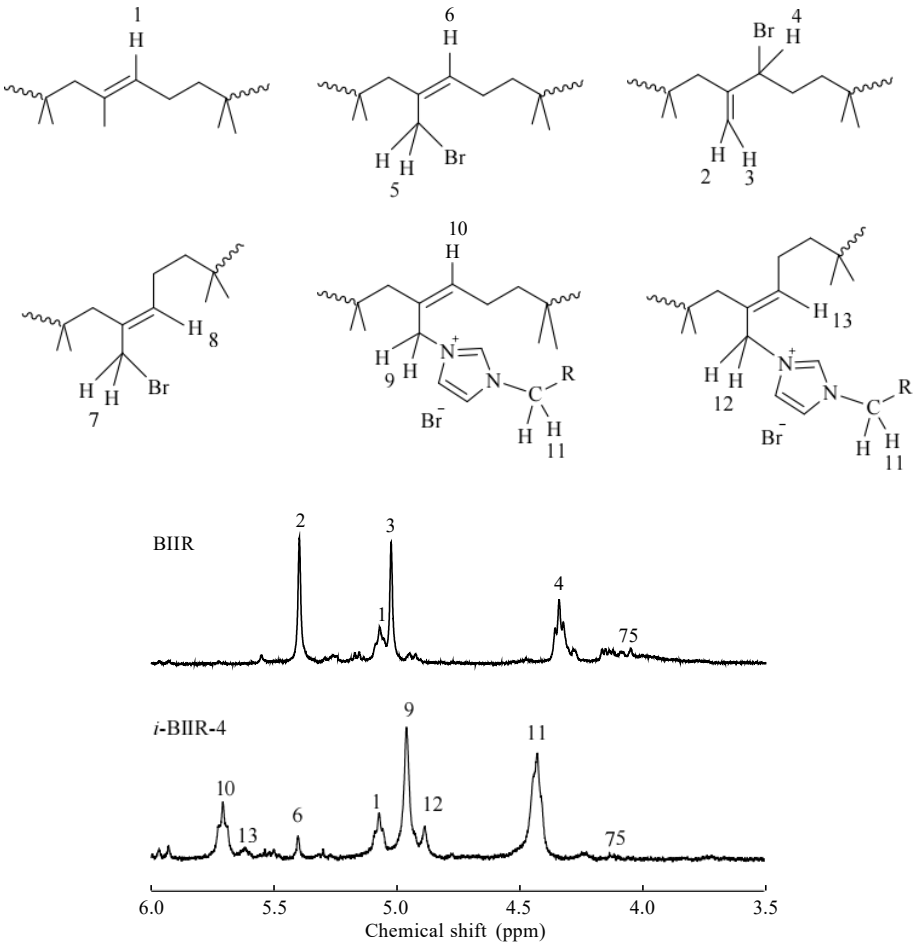

Fig. 1 ^{1}H-NMR spectra of BIIR and *i*-BIIR-4 in $CDCl_3$

Table 1 Signal intensities and conversion of grafting degree

Sample	Signal intensities		Conversion
	H9 + H12 (I = 1) [a]	H5 + H7	
BIIR	–	–	–
i-BIIR-2	1	0.09	0.92
i-BIIR-4	1	0.06	0.94
i-BIIR-8	1	0.10	0.90
i-BIIR-12	1	0.08	0.93

[a] The intensities were set to 1.

−64 °C, a typical value for rubber (Fig. 2a). A new melting point ($T_{m\text{-}ia}$) was observed for the *i*-BIIR. This endothermic transition was interpreted as the melting point of ionic associates[34]. This melting temperature decreased with increasing side chain length because the longer chain may shield ion interactions[39–41]. However, no obvious change was observed for the elastomers after side chain modification. This observation might be due to the low content of Br in BIIR rubber, which resulted in low content of ionic groups. The results of T_g, $T_{m\text{-}ia}$ and the enthalpies of melting ($\Delta H_{m\text{-}ia}$) are listed in Table S1 (in ESI). DMA test is very sensitive to the transition of polymer segments motion. As shown in Fig. 2(b), the broad glass transitions of BIIR and *i*-BIIR occurred on the low temperature side at −47 and −30 °C, corresponding to its special α-relaxation transition peak, respectively[42]. In contrast to the neat BIIR, a new weak relaxation peak appeared above r.t. for *i*-BIIR, which was attributed to the temperature of segmental motion with ion aggregation[43]. For the ionomers, formation of ionic network restricted the mobility of polymer chains, which could have a profound influence on the segment transition of the ionicelastomer. It was observed that the temperature of the relaxation peak decreased with the increasing side chain length. This phenomenon further revealed that the dodecyl chain might easily shield the ion interactions, which was beneficial to segmental motion. These results were in good agreement with the DSC results.

In addition, TGA and rheological tests were also performed to study the thermal processing properties of the samples. All the samples exhibited good thermal stability with a high decomposition temperature around 350 °C in nitrogen (Fig. 2c). As shown in Fig. 2(d), compared with the neat BIIR, the ionic modified elastomers showed a higher viscosity because of the ion associations[33]. Moreover, the *i*-BIIR-2 was found to exhibit the highest viscosity due to the stronger ion associations compared to other ionomers. Ionic aggregates of ionic modified BIIR led to the compact chain structure and physical crosslink networks, resulting in higher viscosity than BIIR.

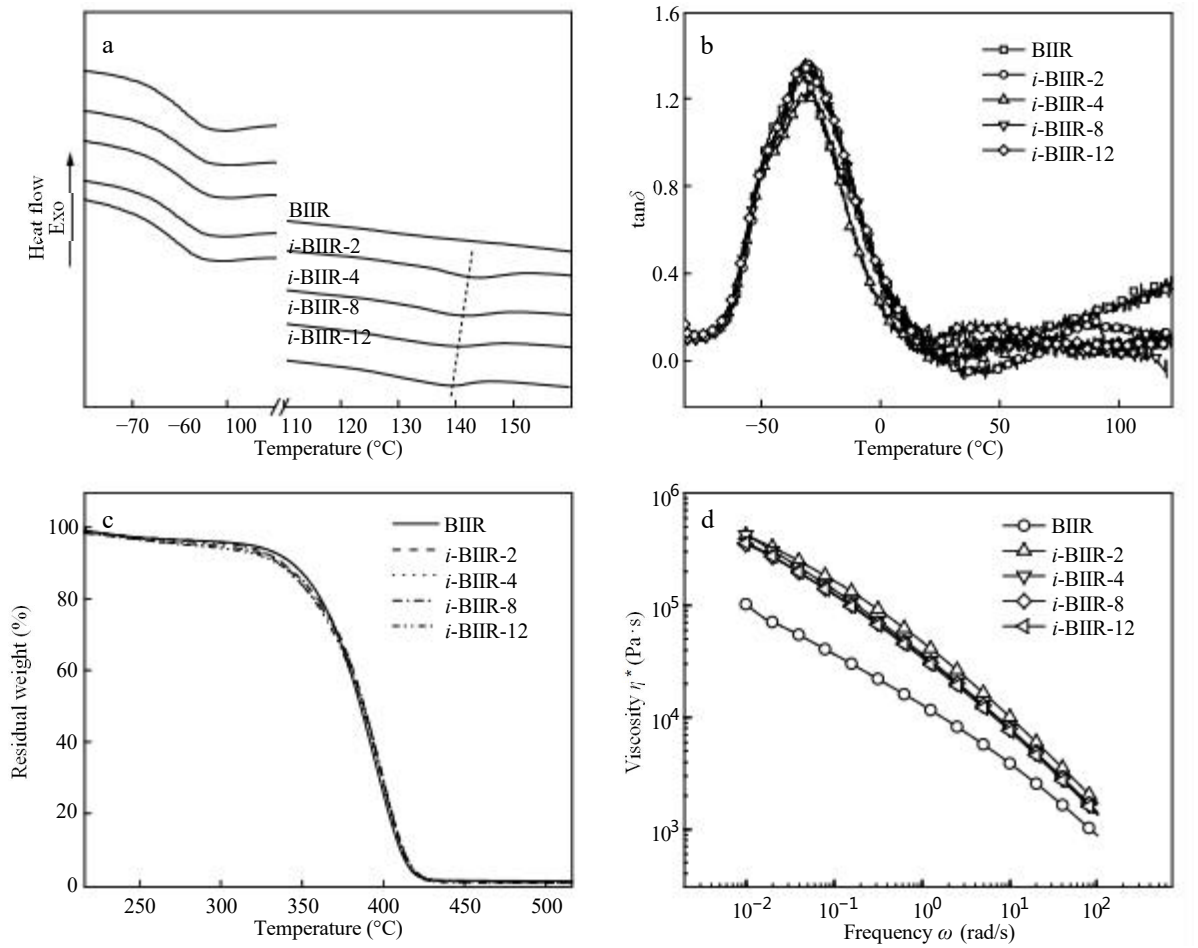

Fig. 2 (a) The DSC heating curves at 10 °C/min, (b) tanδ versus temperature of DMA traces, (c) TGA curves, and (d) complex viscosities of BIIR andall *i*-BIIR ionomers

Miscibility of the PLA/BIIR and PLA/*i*-BIIR Blends

Based on the properties of ionic modified BIIR, a series of PLA melt blending with the BIIR and ionic modified BIIR were conducted to investigate the influence of ionic modification on the PLA/ionic elastomer blends (listed in Table S2 in ESI). The obtained polymer blends were denoted as PLA/*X*%BIIR or PLA/*X*%*i*-BIIR, where *X* represents the weight ratio of *i*-BIIR in the polymer blends. Meanwhile, the 10 wt% content of *i*-BIIR was selected to further explore the impact of the alkyl chain length on properties of the blending materials. DMA analysis was firstly used to analyze the phase miscibility of the blends. The tanδ curves of the neat PLA and PLA/*i*-BIIR-4 blends are shown in Fig. 3. Only one tanδ peak was observed at −76.1 °C for the neat PLA, which was attributed to the glass transition of PLA. For PLA/*i*-BIIR-4 blends, two distinct tanδ peaks were observed, corresponding to the two-component glass transition, respectively. The T_gs of both *i*-BIIR-4 and PLA phases were found to shift toward each other following the increase of *i*-BIIR-4, indicating that *i*-BIIR-4 and PLA were partially miscible. For the PLA/ionic liquid (IL) based blends, several reports pointed out that the existing intermolecular interaction between the anion or cation of IL and ester group of PLA was the main underlying driving force for the miscibility of the blend, like the hydrogen bonding and ion-dipole interactions[18]. The improved miscibility in the present PLA/*i*-BIIR ionomer blend should be also attributed to the intermolecular interaction formed between the PLA and *i*-BIIR phase. Fig. 3(c) shows tanδ versus temperature curves of PLA/*i*-BIIR with different alkyl chain lengths at 10 wt% content. Compared to the blends with the short alkyl chain length *i*-BIIR, the T_gs of two components were found to shift much closer for the PLA/*i*-BIIR-12. This result indicated that the longer alkyl chain with C12 showed better miscibility compared with the *i*-BIIR with short alkyl chain length. As discussed in the previous part, the longer alkyl chain of the *i*-BIIR-12 easily prevented the formation of ionic aggregates inside the elastomer through shielding the internal ion interactions of the elastomer chains. It could be beneficial for interfacial intermolecular interaction between the PLA and ionomeric phase, which was favorable for the miscibility of the blends.

Phase Morphology of the Blends

The phase morphology of polymer blends is closely related to physical properties of polymer blends. Fig. 4 shows the SEM images of the cryo-fractured surfaces of the PLA/*i*-BIIR-4 and PLA/BIIR blends with various blending ratios. A

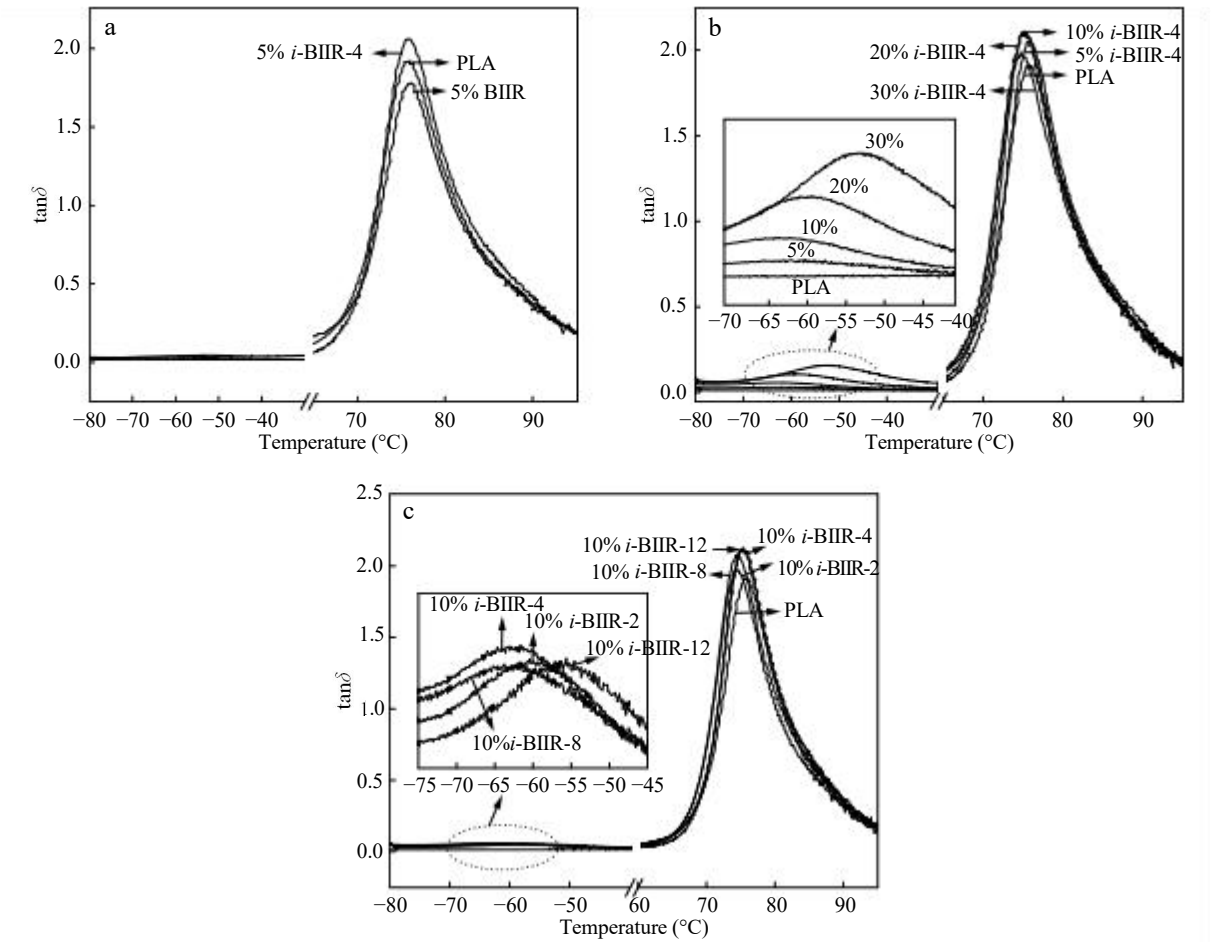

Fig. 3 DMA tanδ versus temperature curves of neat PLA and PLA/*i*-BIIR blends: (a) PLA, PLA/5%BIIR, PLA/5%*i*-BIIR-4; (b) PLA, PLA/*i*-BIIR-4 blends at 5 wt%, 10 wt%, 20 wt%, and 30 wt% contents; (c) PLA, PLA/*i*-BIIR with different alkyl chain lengths at 10 wt% content

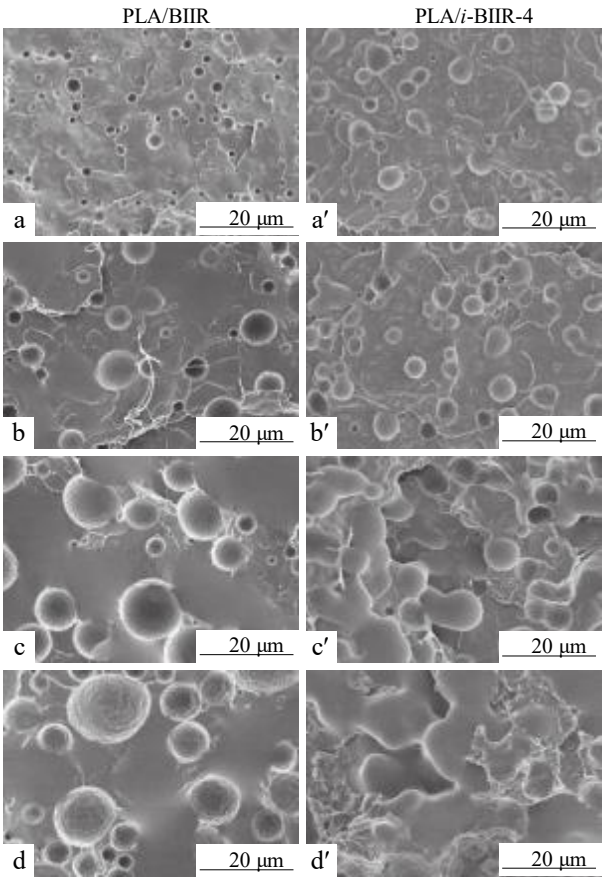

Fig. 4 SEM images taken at cryo-fractured surface of PLA blends with *i*-BIIR-4 or BIIR at various concentrations: (a, a′) 5 wt%, (b, b′) 10 wt%; (c, c′) 20 wt%; (d, d′) 30 wt%

typical phase-separated morphology was observed for all the blends, indicating the limited miscibility of the components. Meanwhile, for the PLA/BIIR blend, some voids were left in the PLA matrix resulting from separation of particles during cold fracture. The clear interface between the PLA matrix and BIIR particles can be attributed to poor interfacial compatibility between the two phases. Compared with the PLA/BIIR blends, some large *i*-BIIR-4 ionomer particles were observed to unevenly disperse in the matrix and the average sizes of those voids (d ~10 μm) increased with the increasing content of ionic elastomer. Even slightly semi-continuous phase was formed in the case of PLA/30%*i*-BIIR-4 blends. However, it was noted that the dispersed *i*-BIIR-4 particles were well-imbedded in the PLA matrix with better interfacial adhesion than that of PLA/BIIR blend, which implied a better interfacial compatibility between the PLA and *i*-BIIR phases. It is well-known that the phase morphology of dispersed phase in polymer blend is determined by multiple factors including composition, viscosity-ratio and miscibility of the components[13, 44, 45]. As mentioned in the previous part, the introduction of ionic group in the modified BIIR could lead to a higher viscosity compared with the BIIR, especially for the ionomer with short alkyl chain length. In addition, the compact chain structure in the ionomer with short alkyl chain length would form short-range interaction in the ionic aggregation more easily, which is difficult to interact with other phases. Consequently, for the PLA/*i*-BIIR-4 with a short alkyl chain length, although the interfacial compatibility was improved, the increasing viscosity might play a dominant role in determining the phase structure of the blend. Considering the shielding effect of longer alkyl chain length and low viscosity of the elastomer, the PLA/*i*-BIIR with a longer alkyl chain length would possess better compatibility. Fig. 5 presents the phase morphologies of the PLA/*i*-BIIR with different alkyl chain lengths. It can be clearly noted that the PLA/*i*-BIIR-12 blend with longer alkyl chain length showed more uniform dispersion of dispersed phase and better interfacial adhesion compared with that of the PLA/*i*-BIIR with short alkyl chain length. These results further proved the previous analysis and conclusion from the DMA results.

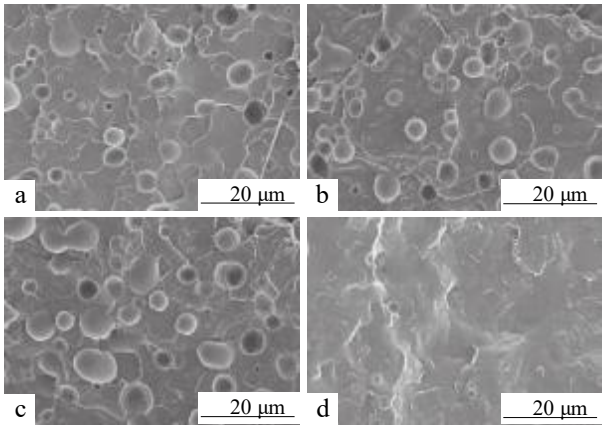

Fig. 5 SEM images taken at cryo-fracture surface of (a) PLA/10%*i*-BIIR-2, (b) PLA/10%*i*-BIIR-4, (c) PLA/10%*i*-BIIR-8, (d) PLA/10%*i*-BIIR-12

Thermal and Crystallization Behaviors

PLA is a kind of typical semi-crystalline polymer, and its physical properties strongly depend on its crystallization behavior. The crystallization and melting behaviors of the PLA component in the blends were characterized by DSC, and the heating curves of the neat PLA and blend are shown in Fig. 6. The detail results of the thermal and crystallization properties of blends are listed in Table S3 (in ESI). In consistent with the DMA results, no obvious change was observed for the glass transition behavior of the PLA/BIIR blend. A slight decrease could be observed for T_g of the PLA/*i*-BIIR blends, suggesting some level of improved miscibility resulting from the intermolecular interaction between the phases. When 5 wt% contents of elastomer were incorporated into the PLA matrix, a clear decrease of cold crystallization temperature (T_{cc}) was observed for both the PLA/BIIR and PLA/*i*-BIIR blends. The maximum degrees of crystallinity of PLA/BIIR and PLA/*i*-BIIR-4 were 8.23% and 8.70% at 10 wt% content and 5 wt% content, respectively. These results demonstrated that the dispersed elastomer particles played a nucleating role for PLA in the blend. However, it is interesting to note that the T_{cc} of the PLA/BIIR blends increased with the content of BIIR increasing. When BIIR content was up to 30 wt%, the T_{cc} decreased again. This result may be related to the dilution

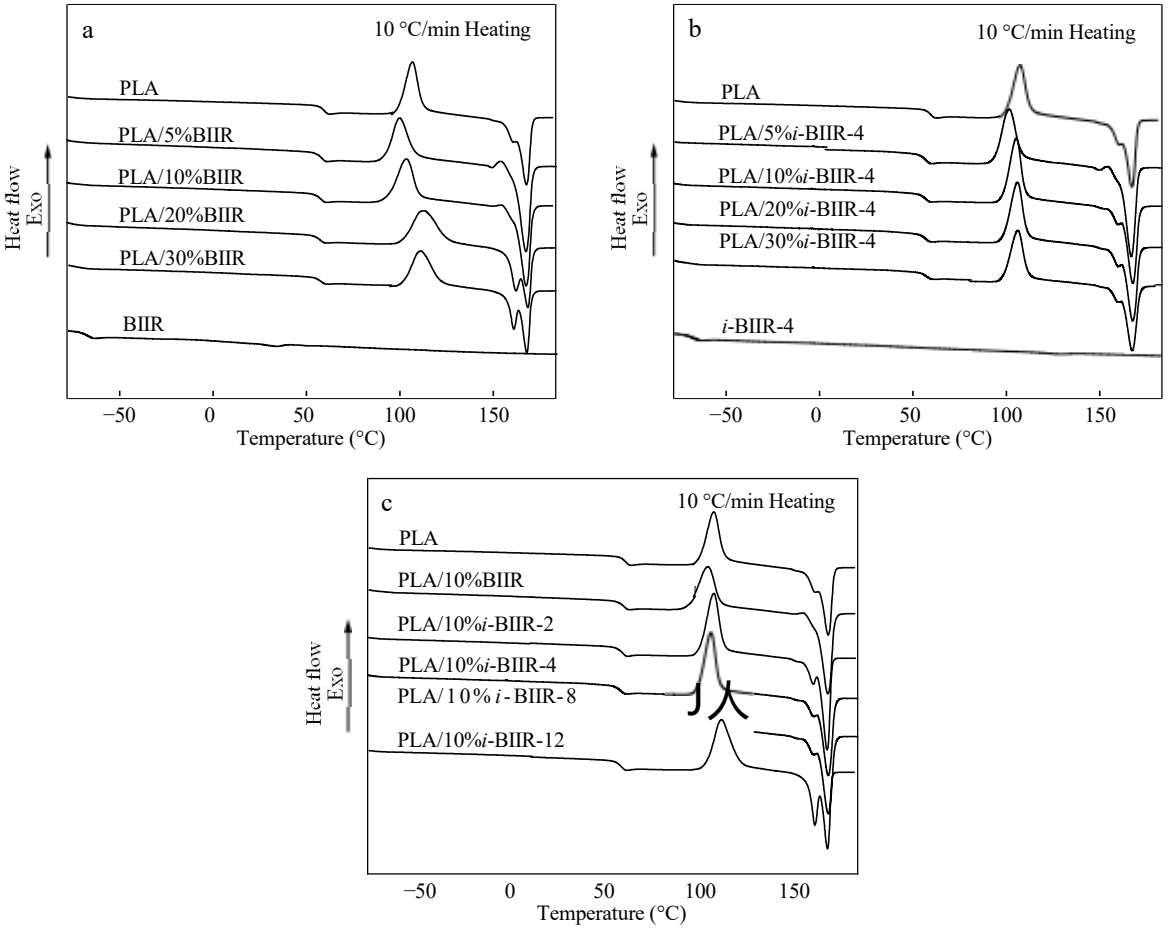

Fig. 6 DSC heating curves of the neat PLA and the blends with BIIR and *i*-BIIR: (a) PLA/BIIR blends, (b) PLA/*i*-BIIR-4 blends, (c) PLA/10%BIIR and PLA/10%*i*-BIIR blends with alkyl chain of different lengths

effect of the BIIR as an amorphous polymer component in the PLA matrix. At the same time, larger rubber phase particles were also demonstrated in the SEM results, which would also be disadvantageous for the nucleation. In the contrary, no evident changes were found for the PLA/*i*-BIIR-4 blend. This difference between the PLA/BIIR and PLA/*i*-BIIR-4 blends may be related to the different compatibility of the components. Because of the poor miscibility of PLA and BIIR, the nucleating role was weakened for the PLA/BIIR blends with the content of elastomer increasing. However, for PLA/*i*-BIIR blend with better interfacial adhesion, the nucleating role was retained owing to the improved compatibility[11, 46, 47]. For the polymer blend, the nucleating role and dilution effect of dispersed component played an opposite effect on the crystallization of polymer matrix. As shown in Fig. 6(c), when the miscibility was further enhanced for the PLA/*i*-BIIR-12 with longer alkyl chain length, the dilution effect played a dominant role because of the enhancing compatibility, resulting in an increase of the T_{cc}.

Mechanical Properties of the Blends

Poor flexibility and toughness are the main bottlenecks that limit the wide applications of PLA materials. The mechanical properties of the PLA/BIIR and PLA/*i*-BIIR blends were studied by tensile test and notched Izod impact test. Fig. 7 presents the typical stress-strain curves of PLA/elastomer blends reasonably selected based on the average value. Neat PLA is a typically brittle and stiff material with an elongation at break of only 23% and tensile strength of about 69 MPa. When BIIR was added into the PLA matrix, the yield stress of the sample gradually decreased, while the elongation at break reached the maximum at 10 wt% content (up to 65%) and then decreased gradually. For the PLA/*i*-BIIR-4 blends, with the addition of 10 wt% *i*-BIIR-4, the blend showed the largest elongation at break up to 110%, which is 6 times of the original value of the neat PLA, while the tensile strength remained at 48 MPa. The improved flexibility of PLA/*i*-BIIR-4 blends may be attributed to their better compatibility compared with that of the PLA/BIIR blend. All the blend samples showed the cold-drawing behavior under tensile stretch. Obvious stress platform of plastic deformation after the yield point, accompanied by necking shrinkage and stress whitening phenomenon, was observed for the blend samples resulting from the shear yielding during the tensile test. As the content of *i*-BIIR-4 increased up to 20 wt%, the elongation at break of the blend decreased to 85%, which increased by about 4 times than that of neat PLA. When the *i*-BIIR-4 content increased to 30 wt%, the elongation at break and the tensile strength decreased due to semi-continuous phase structure and dilution effect of rubber as a

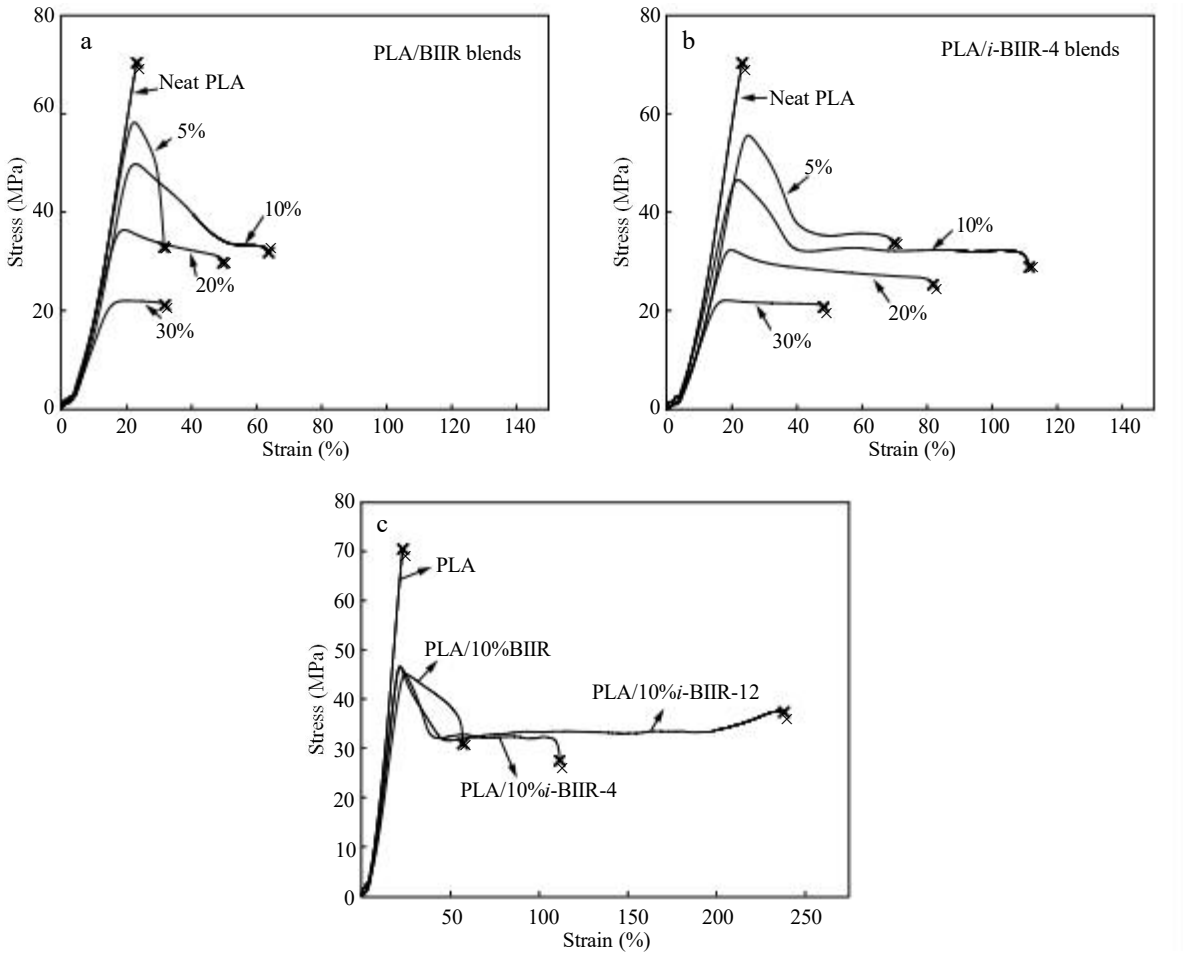

Fig. 7 Tensile stress-strain curves of the neat PLA and the blends with BIIR or *i*-BIIR: (a) PLA/BIIR blends, (b) PLA/*i*-BIIR-4 blends, (c) PLA/10%BIIR, PLA/10%*i*-BIIR-4 and PLA/10%*i*-BIIR-12

heterogeneous component. Fig. 7(c) shows the summarized typical tensile stress-strain curves of PLA/*i*-BIIR blends with different alkyl chain lengths. Compared with neat PLA and PLA/BIIR blend, there was a significant increase in the elongation at break for the PLA/*i*-BIIR-12 at a value of 235%, almost 10 times higher than that of neat PLA. Moreover, no clear sacrificing in the tensile strength was observed compared with that of other formulation. This excellent mechanical performance was attributed to the improved interfacial compatibility between PLA and *i*-BIIR-12 grafted with longer chain. The higher tensile strength of the PLA blend with ionic-modified BIIR may be due to the formed intermolecular interaction between the ions (*i.e.*, imidazolium cation and bromide anion) in ionic-modified BIIR and ester group of PLA[8, 25]. The results clearly showed that the ionic-modified BIIR with longer alkyl chain length was a very effective toughening agent to improve the ductile properties of PLA.

Impact strength is another important mechanical property of PLA materials. Based on the tensile tests, typical impact strength of PLA/elastomeric ionomers blends (90/10) with different alkyl chain lengths was characterized through the notched Izod impact strength test,and the results are summarized in Fig. 8. As shown in Fig. 8, the addition of

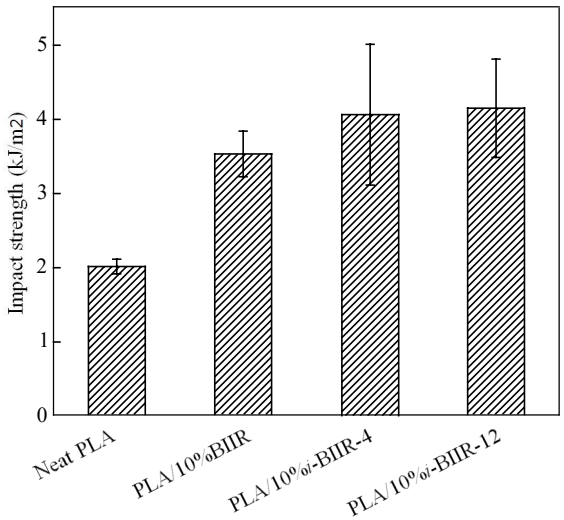

Fig. 8 Impact strength of the neat PLA and PLA blends with BIIR, *i*-BIIR-4 and *i*-BIIR-12 at 10 wt%

10 wt% BIIR and ionic-modified BIIR improved the impact strength of PLA. PLA/*i*-BIIR-12 showed the optimum toughness with the impact strength of 4.1 kJ/m^2. This result was inconsistent with the tensile property.

Toughening Mechanism

The impact strength of the material is normally determined by the combination of compatibility, dispersion state and size of the disperse phase in matrix. It is well-known that suitable interfacial bonding and good dispersion of the disperse phase in matrix are the critical factors to achieve high toughness of polymer and rubber blend[13, 14, 48]. To figure out the intrinsic toughening mechanism in the PLA/BIIR-based blend, we investigated the impact fracture surfaces of the typical impact samples through the SEM observation, as shown in Fig. 9. Neat PLA showed typical brittle fracture characteristics with a smooth and flat broken surface. The addition of BIIR-based elastomer effectively enhanced the impact strength of PLA. Accordingly, rough surfaces were seen for the PLA/BIIR-based blends. However, some voids were observed in the PLA/BIIR blend *via* an in-depth analysis of the surfaces of PLA/BIIR, indicating the very limited compatibility between the phases. In contrast to what was shown in the PLA/BIIR blend, well-embedded particles in the PLA matrix were clearly found in the PLA/*i*-BIIR-4 blend, which is an evidence of good interfacial adhesion. A coarser surface with some lamellar-like multiple fracture deformation was further formed for the PLA/*i*-BIIR-12 besides the well-embedded particles, suggesting a better interfacial adhesion performance. It was well accepted that matrix shear deforming, which was triggered by microvoiding derived from interfacial debonding or internal cavitation of dispersedelastomer particles, was the main toughening mechanism in rubber-toughened polymer blend[49, 50]. For present PLA/BIIR-based elastomer blend with limited miscibility, interfacial debonding possibly was a predominant mechanism and essential step for improving toughness of the blends. A suitable interfacial adhesion is a key factor for achieving the desirable toughness. Poor interfacial bonding is liable to too strong adhesion may restrict debonding, which will be unfavorable for initiating matrix yielding[18, 21–23]. For the PLA/BIIR and PLA/*i*-BIIR-4 blends, the limited interfacial adhesion was not strong enough to resist the crack propagation, resulting in unsatisfied toughening effect. However, the better compatibility of *i*-BIIR-12 with PLA matrix was beneficial for initiating matrix deforming, thereby resulting inconsiderable energy dissipation.

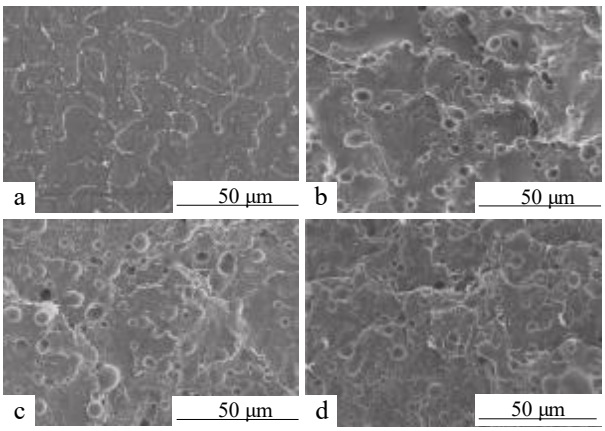

Fig. 9 SEM images of impact-fracture surface of (a) the neat PLA and PLA blends with (b) BIIR, (c) *i*-BIIR-4 and (d) *i*-BIIR-12 at 10 wt%

CONCLUSIONS

In the present work, we synthesized a series of ionically modified BIIR containing different alkyl imidazolium chains to construct a novel ductile PLA blend system. We successfully obtained the modified BIIR with ≥ 0.90 grafting degree. The *i*-BIIR exhibited good mechanical property, thermal stability and processing performance, which was an ideal modifier for melt blending with PLA. Compared with the PLA/unmodified BIIR blend, the PLA/*i*-BIIR ionomers blends exhibited better compatibility due to the presence of intermolecular interaction. Significant enhancement of the flexibility of the PLA was gained for the PLA/BIIR-ionomer blend. In particular, an excellent elongation at break up to 235% was achieved for the blends using the *i*-BIIR ionomer with longer alkyl chain. Impact-fracture morphologies indicated that a suitable phase structure with the optimum interfacial adhesion played a vital role in improving the toughness of the PLA/*i*-BIIR blends. The fact that microvoids were first formed from interfacial debonding and then triggered the yielding of the surrounding matrix implied the dominant toughening mechanism in the blends with suitable intermolecular interactions. This paper describes a promising example of compatibilization and toughening of the PLA blend by introducing the organic ionic elastomeric ionomer. Future work will focus on developing super-toughening PLA materials without sacrificing the advantages of PLA by optimizing chain structure and increasing the contents of ionic group.

1 Chen, G. Q.; Patel, M. K. Plastics derived from biological sources: present and future: a technical and environmental review. Chem. Rev. 2012, 112(4), 2082−2099.

2 Zhang, X. Y.; Fevre, M.; Jones, G. O.; Waymouth, R. M. Catalysis as an enabling science for sustainable polymers.

Chem. Rev. 2018, 118(2), 839−885.
3 Auras, R.; Harte, B.; Selke, S. An overview of polylactides as packaging materials. Macromol. Biosci. 2004, 4(9), 835−864.
4 Farah, S.; Anderson, D. G.; Langer, R. Physical and mechanical properties of PLA, and their functions in widespread applications - a comprehensive review. Adv. Drug Deliv. Rev. 2016, 107(21), 367−392.
5 Hou, J. Z.; Sun, X. P.; Zhang, W. X.; Li, L. L.; Teng, H. Preparation and characterization of electrospun fibers based on poly(L-lactic acid)/cellulose acetate. Chinese J. Polym. Sci. 2012, 30(6), 916−922.
6 Yao, C.; Li, X. S.; Neoh, K. G.; Shi, Z. L.; Kang, E. T. Antibacterial poly(D,L-lactide) (PDLLA) fibrous membranes modified with quaternary ammonium moieties. Chinese J. Polym. Sci. 2010, 28(4), 581−588.
7 Wu, N. J.; Zhang, H.; Fu, G. L. Super-tough poly(lactide) thermoplastic vulcanizates based on modified natural rubber. ACS Sustain. Chem. Eng. 2017, 5(1), 78−84.
8 Wang, P.; Xu, P.; Wei, H. B.; Fang, H. G.; Ding, Y. S. Effect of block copolymer containing ionic liquid moiety on interfacial polarization in PLA/PCL blends. J. Appl. Polym. Sci. 2018, 10.1002/APP.46161.
9 Delgado, P. A.; Hillmyer, M. A. Combining block copolymers and hydrogen bonding for poly(lactide) toughening. RSC Adv. 2014, 4(26), 13266−13273.
10 Hao, Y. P.; Ge, H. H.; Han, L. J.; Zhang, H. L.; Dong, L. S.; Sun, S. L. Thermal and mechanical properties of polylactide toughened with a butyl acrylate-ethyl acrylate-glysidyl methacrylate copolymer. Chinese J. Polym. Sci. 2013, 31(11), 1519−1527.
11 Zhang, K. Toughened sustainable green composites from poly(3-hydroxybutyrate-*co*-3-hydroxyvalerate) based ternary blends and miscanthus biofiber. ACS Sustain. Chem. Eng. 2014, 2(10), 2345−2354.
12 Yu, R. L.; Zhang, L. S.; Feng, Y. H.; Zhang, R. Y.; Zhu, J. Improvement in toughness of polylactide by melt blending with bio-based poly(ester)urethane. Chinese J. Polym. Sci. 2014, 32(8), 1099−1110.
13 Xing, Q.; Li, R. B.; Dong, X.; Zhang, X. Q.; Zhang, L. Y.; Wang, D. J. Phase morphology, crystallization behavior and mechanical properties of poly(L-lactide) toughened with biodegradable polyurethane: effect of composition and hard segment ratio. Chinese J. Polym. Sci. 2015, 33(9), 1294−1304.
14 Zhang, K. Y.; Ran, X. H.; Wang, X. M.; Han, C. Y.; Han, L. J.; Wen, X.; Zhuang, Y. G.; Dong, L. S. Improvement in toughness and crystallization of poly(L-lactic acid) by melt blending with poly(epichlorohydrin-*co*-ethylene oxide). Polym. Eng. Sci. 2011, 51(12), 2370−2380.
15 Yuan, D. S.; Chen, Z. H.; Xu, C. H.; Chen, K. L.; Chen, Y. K. Fully biobased shape memory material based on novel cocontinuous structure in poly(lactic acid)/natural rubber TPVs fabricated via peroxide-induced dynamic vulcanization and in situ interfacial compatibilization. ACS Sustain. Chem. Eng. 2015, 3(11), 2856−2865.
16 Zhang, K. Y.; Nagarajan, V.; Misra, M.; Mohanty, A. K. Supertoughened renewable PLA reactive multiphase blends system: phase morphology and performance. ACS Appl. Mater. Interfaces 2014, 6(15), 12436−12448.
17 Dong, W. Y.; He, M. F.; Wang, H. T.; Ren, F. L.; Zhang, J. Q.; Zhao, X. W.; Li, Y. J. PLLA/ABS blends compatibilized by reactive comb polymers: double T_g depression and significantly improved toughness. ACS Sustain. Chem. Eng. 2015, 3(10), 2542−2550.
18 Lin, Y.; Zhang, K. Y.; Dong, Z. M.; Dong, L. S.; Li, Y. S. Study of hydrogen-bonded blend of polylactide with biodegradable hyperbranched poly(ester amide). Macromolecules 2007, 40(17), 6257−6267.
19 Han, S. I.; Yoo, Y. T; Kim, D. K.; Im, S. S. Biodegradable aliphatic polyester ionomers. Macromol. Biosci. 2004, 4(3), 199−207.
20 Park, S. B.; Hwang, S. Y.; Moon, C. W.; Im, S. S. Plasticizer effect of novel PBS ionomer in PLA/PBS ionomer blends. Macromol. Res. 2010, 18(5), 463−471.
21 Liu, H. Z.; Chen, F.; Liu, B.; Estep, G.; Zhang, J. W. Super toughened poly(lactic acid) ternary blends by simultaneous dynamic vulcanization and interfacial compatibilization. Macromolecules 2010, 43(14), 6058−6066.
22 Liu, H. Z.; Song, W. J.; Chen, F.; Guo, L.; Zhang, J. W. Interaction of microstructure and interfacial adhesion on impact performance of polylactide (PLA) ternary blends. Macromolecules 2011, 44(6), 1513−1522.
23 Liu, H. Z.; Guo, X. J.; Song, W. J.; Zhang, J. W. Effects of metal ion type on ionomer-assisted reactive toughening of poly(lactic acid). Ind. Eng. Chem.Res. 2013, 52(13), 4787−4793.
24 Megevand, B.; Pruvost, S.; Lins, L. C.; Livil, S.; Gérard, J. F.; Duchet-Rumeau, J. Probing nanomechanical properties with AFM to understand the structure and behavior of polymer blends compatibilized with ionic liquids. RSC Adv. 2016, 6(98), 96421−96430.
25 Lins, L. C.; Livi, S.; Duchet-Rumeau, J.; Gérard, J. F. Phosphonium ionic liquids as new compatibilizing agents of biopolymer blends composed of poly(butylene-adipate-*co*-terephtalate)/poly(lactic acid) (PBAT/PLA). RSC Adv. 2015, 5(73), 59082−59092.
26 Wang, P.; Zhang, D.; Zhou, Y. Y.; Li, Y.; Fang, H. G.; Wei, H. B.; Ding, Y. S. A well-defined biodegradable 1,2,3-triazolium-functionalized PEG-*b*-PCL block copolymer: facile synthesis and its compatibilization for PLA/PCL blends. Ionics 2018, 10.1007/s11581-017-2234-3.
27 Jérémy, O.; Jean-Marie, R.; Cédric, S.; Sophie, B.; Apostolos, E.; Dubois, P.; Giannelis, E. P. Shape-memory behavior of polylactide/silica ionic hybrids. Macromolecules 2017, 50(7), 2896−2905.
28 Livi, S.; Duchet-Rumeau, J.; Gérard, J. F.; Pham, T. N. Polymers and ionic liquids: a successful wedding. Macromol. Chem. Phys. 2015, 216(4), 359−368.
29 Chen, B. K.; Wu, T. Y.; Chang, Y. M.; Chen, A. F. Ductile polylactic acid prepared with ionic liquids. Chem. Eng. J. 2013, 215-216, 886−893.
30 Gardella, L.; Furfaro, D.; Galimberti, M.; Monticelli, O. On the development of facile approach based on the use of ionic liquids: preparation of PLLA (sc-PLA)/high surface area nano-graphite systems. Green Chem. 2015, 17(7), 4082−4088.
31 Cui, J.; Nie, F. M.; Yang, J. X.; Pan, L.; Ma, Z.; Li, Y. S. Novel imidazolium-Based poly(ionic liquid)s with different counter ions for self-healing. J. Mater. Chem. A 2017, 5, 25220−25229.
32 Le, H. H.; Das, A. Triggering the self-healing properties of modifed bromobutyl rubber by intrinsically electrical heating. Macromol. Mater. Eng. 2017, 302, 1600385.
33 Das, A.; Sallat, A.; Böhme, F.; Suckow, M.; Basu, D.; Wießner, S.; Stöckelhuber, K. W.; Voit, B.; Heirich, G. Ionic modification turns commercial rubber into a self-healing material. ACS Appl. Mater. Interfaces 2015, 7(37), 20623−20630.
34 Suckow, M.; Mordvinkin, A.; Roy, M.; Singha, N. K.; Heinrich, G.; Voit, B.; Saalwächter, K.; Böhme, F. Tuning the properties and self-healing behavior of ionically modified poly(isobutylene-*co*-isoprene) rubber. Macromolecules 2018, 51(2), 468−479.
35 Meng, Q. Q.; Wang, B.; Pan, L.; Li, Y. S.; Ma, Z. Synthesis and properties of isotactic polypropylene ionomers containing ammonium Ions. Acta Polymerica Sinica (in Chinese) 2017, 11, 1762−1772.
36 Lee, M.; Choi, U. H.; Wi, S.; Slebodnick, C.; Colby, R. H.; Gibson, H. W. 1,2-Bis[*N*-(*N*′-alkylimidazolium)] ethane salts: a new class of organic ionic plastic crystals. J. Mater. Chem.

2011, 21(33), 12280−12287.
37 Dakin, J. M.; Shanmugam, K. V. S.; Twigg, C.; Whitney, R. A.; Parent, J. S. Isobutylene-rich macromonomers: dynamics and yields of peroxide-initiated crosslinking. Polym. Chem. 2015, 53(1), 123−132.
38 Parent, J. S.; Porter, A. M. J.; Kleczek, M. R.; Whitney, R. A. Imidazolium bromide derivatives of poly(isobutylene-*co*-isoprene): a new class of elastomeric ionomers. Polymer 2011, 52(24), 5410−5418.
39 Kim, A.; Miller, K. M. Synthesis and thermal analysis of crosslinked imidazolium-containing polyester networks prepared by Michael addition polymerization. Polymer 2012, 53(25), 5666−5674.
40 Ye, Y. S.; Sharick, S.; Davis, E. M.; Winey, K. I.; Elabd, Y. A. High hydroxide conductivity in polymerized ionic liquid block copolymers. ACS Macro Lett. 2013, 2(7), 575−580.
41 Nykaza, J. R.; Ye, Y. S.; Elabd, Y. A. Polymerized ionic liquid diblock copolymers with long alkyl side-chain length. Polymer 2014, 55(16), 3360−3369.
42 Wu, J. R.; Huang, G. S.; Pan, Q. Y.; Zheng, J.; Zhu, Y. C.; Wang, B. An investigation on the molecular mobility through the glass transition of chlorinated butyl rubber. Polymer 2007, 48(26), 7653−7659.
43 Mora-Barrantes, I.; Malmierica, M. A.; Valentin, J. L.; Rodriguez, A.; Ibarra, L. Effect of covalent cross-links on the network structure of thermo-reversible ionic elastomers. Soft Matter 2012, 8(19), 5201−5213.
44 Marin, N.; Favis, B. D. Co-continuous morphology development in partially miscible PMMA/PC blends. Polymer 2002, 43(17), 4723−4731.
45 Harrats, C.; Thomas, S. and Groeninckx, G. "Micro- and nanostructured multiphase polymer blends system", CRC Press, 2006, p. 4-33.
46 Phetwarotai, W.; Tanrattanakul, V.; Phusunti, N. Synergistic effect of nucleation and compatibilization on the polylactide and poly(butylene adipate-*co*-terephthalate) blend films. Chinese J. Polym. Sci. 2016, 34(9), 1129−1140.
47 Nagarajan, V Overc.oming the fundamental challenges in improving the impact strength and crystallinity of PLA biocomposites: influence of nucleating agent and mold temperature. ACS Appl. Mater. Interfaces 2015, 7(21), 11203−11214.
48 Yu, F.; Huang, H. X. Simultaneously toughening and reinforcing poly(lactic acid)/thermoplastic polyurethane blend *via* enhancing interfacial adhesion by hydrophobic silica nanoparticles. Polym. Test. 2015, 45, 107−113.
49 Zhang, K. Y.; Mohanty, A. K.; Misra, M. Fully biodegradable and biorenewable ternary blends from polylactide, poly(3-hydroxybutyrate-*co*-hydroxyvalerate) and poly(butylene succinate) with balanced properties. ACS Appl. Mater. Interfaces 2012, 4(6), 3091−3101.
50 Zhang, K. Y.; Nagarajan, V.; Misra, M.; Mohanty, A. K. Super toughened renewable PLA reactive multiphase blends system: phase morphology and performance. ACS Appl. Mater. Interfaces 2014, 6(15), 12436−12448.